The structure–property relationships in M-type hexaferrites: Hyperfine interactions and bulk magnetic properties

G. K. Thompson and B. J. Evans
Department of Chemistry, University of Michigan, Ann Arbor, Michigan 48109-1055

^{57}Fe Mössbauer spectroscopic measurements have been made at 296 K on single crystals of $MFe_{12}O_{19}$ (M=Ba, Sr, Pb) oriented parallel and perpendicular to the *c* axis, permitting the establishment of the systematics of the static and dynamical aspects of the hyperfine interactions, and their relationship to crystal/chemical structures for the five Fe^{3+} sublattices, and to the bulk magnetic properties. With the exception of the electric quadrupole interaction at the 2*b* site, and the dependence of the 2*b* intensity on the crystal orientation, the magnitude of the hyperfine interactions of a given Fe^{3+} site exhibits only small variations among the different hexaferrites. The magnitude of the quadrupole interaction at the 2*b* site varies by more than 10%, with the 2*b* site in $PbFe_{12}O_{19}$ exhibiting the smallest value. The relative intensity of the 2*b* subspectrum varies markedly among the three hexaferrites for observations parallel and perpendicular to the *c* axis. Although all display the expected anisotropy resulting from the libration of the 2*b* Fe^{3+} parallel to the *c* axis, the anisotropy is considerably larger for $PbFe_{12}O_{19}$ than for $BaFe_{12}O_{19}$ or $SrFe_{12}O_{19}$. It is remarkable that the bulk magnetic anisotropy follows the same order as the anisotropy in the dynamical displacement and crystalline electric field of the 2*b* site.

I. INTRODUCTION

The M-type hexaferrites, $MFe_{12}O_{19}$ (M=Ba, Sr, Pb), are an important class of ferrimagnetic oxides. Their magnetic properties make them excellent materials for use as permanent magnets, recording media, and as components in microwave and higher-frequency devices.

The structure of these ferrites may be considered to consist of alternating spinel ($S=Fe_6O_8^{2+}$) and hexagonal ($R=MFe_6O_{11}^{2-}$) layers. The O^{2-} ions exist as close-packed layers, with the M^{2+} substituting for an O^{2-} in the hexagonal layer. The Fe^{3+} ions are distributed in the interstitial spaces of the close-packed layers. Three of the Fe^{3+} sites are octahedral (12*k*, $4f_2$, and 2*a*); one is tetrahedral ($4f_1$), and one is trigonal bipyramidal (2*b*).

In previous investigations, single-crystal ^{57}Fe Mössbauer spectroscopy and x-ray diffraction measurements were employed to investigate the dynamics of the 2*b* Fe^{3+} ion in $BaFe_{12}O_{19}$ (Refs. 1–5), $SrFe_{12}O_{19}$ (Refs. 3, 6–8), and $PbFe_{12}O_{19}$.[9,10] However, quantitative and comparative data on the vibrational anisotropy of *all* the Fe^{3+} ions in the end-member hexaferrites, and on their respective hyperfine interaction parameters have been lacking.

Therefore, to determine what influence each of the five Fe^{3+} sites has on the bulk magnetic properties of the different $MFe_{12}O_{19}$ compounds, Mössbauer spectra have been obtained at 296 K for single crystals with the *c* axis parallel and perpendicular to the γ-ray propagation direction.

II. EXPERIMENT

^{57}Fe Mössbauer spectra were collected at 296 K for oriented single crystals of $BaMn_{0.3}Fe_{11.7}O_{19}$, $SrFe_{12}O_{19}$, and $PbFe_{12}O_{19}$. The resulting hyperfine parameters have been compared with the parameters of polycrystalline $BaFe_{12}O_{19}$, $SrFe_{12}O_{19}$, and $PbFe_{12}O_{19}$ reported in an earlier study from this laboratory.[10] The spectra were obtained and analyzed as described in detail in a previous report.[11] Electron microprobe analysis (EMPA) and x-ray powder diffraction were employed to determine the composition and purity of the samples.

III. RESULTS AND DISCUSSION

The spectra for the case in which the *c* axis is perpendicular to the γ-ray propagation direction are quite similar for all samples. A typical spectrum for this orientation, that of $SrFe_{12}O_{19}$, is shown in Fig. 1, along with the spectrum of a polycrystalline sample for comparison. The hyperfine parameters of all the single-crystal samples are listed in Tables I–III. In this orientation, except for $SrFe_{12}O_{19}$, the relative intensity of the 2*b* subspectrum for each of the samples is fairly close to the theoretical value of 2, where the 12*k* site has a normalized intensity of 12 (Tables I–III). For a given Fe^{3+} site, the hyperfine parameters exhibit, *with few exceptions*, no significant variations between the hexaferrites.

The first exception is the unusually large isomer shift of the 2*a* subspectrum of $SrFe_{12}O_{19}$, relative to the other hexaferrites (Tables I–III). This deviation may be due to the difficulty in resolving the $4f_1$ and 2*a* components. The *second exception* is in the high values of the quadrupole interaction of the $4f_1$ and 2*a* sites in $BaMn_{0.3}Fe_{11.7}O_{19}$ (Fig. 2). These larger than normal quadrupole interactions may be due to Jahn–Teller distortions, which have been observed in polycrystalline $BaMn_xFe_{12-x}O_{19}$.[12]

It is notable that, except for the 2*b* site, the electric quadrupole interactions in $SrFe_{12}O_{19}$ and $PbFe_{12}O_{19}$ are very similar for all the iron sites. The quadrupole interaction for the 2*b* site in $SrFe_{12}O_{19}$ is 2.28 mm s^{-1}, versus 2.00 mm s^{-1} for $PbFe_{12}O_{19}$. A comparison of the electric quad-

 0021-8979/93/106295-03$06.00

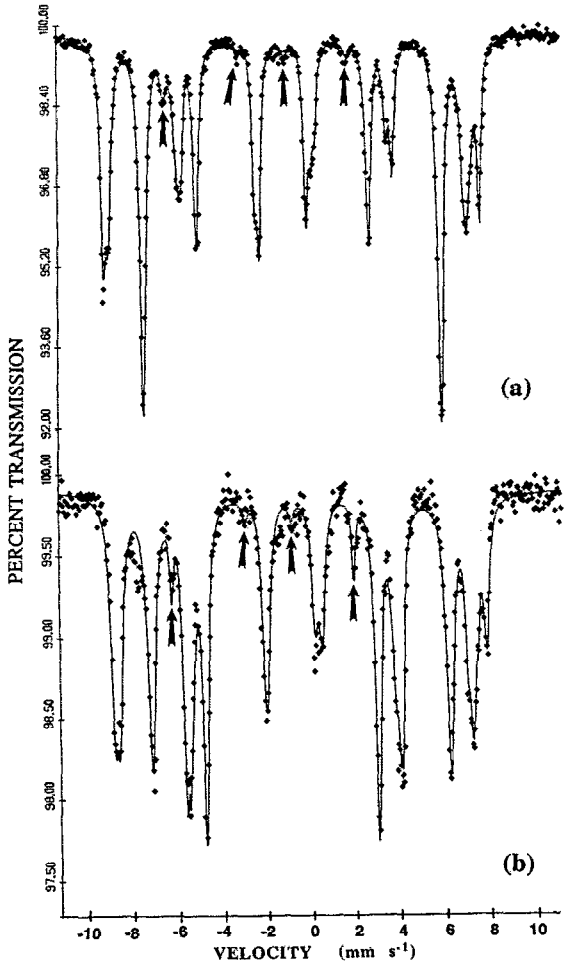

FIG. 1. (a) ^{57}Fe Mössbauer spectrum of polycrystalline $SrFe_{12}O_{19}$ at 296 K. (b) ^{57}Fe Mössbauer spectrum of single-crystal $SrFe_{12}O_{19}$ (c axis perpendicular to γ-ray beam) at 296 K. Arrows in (a) and (b) indicate the $2b$ subspectrum.

TABLE II. ^{57}Fe hyperfine parameters for single-crystal $SrFe_{12}O_{19}$ at 296 K.

Fe^{3+} site	Crystal alignment	H_{eff}[a] (kOe)	Δ[a] (mm s^{-1})	δ[a] (mm s^{-1})	Relative intensity
$12k$	$c\perp$ γ-ray	411	0.42	0.36	12
	$c\parallel$ γ-ray	410	0.51	0.34	12
$4f_2$	$c\perp$ γ-ray	515	0.28	0.41	5.8
	$c\parallel$ γ-ray	511	0.57	0.43	4.9
$4f_1$	$c\perp$ γ-ray	487	0.12	0.30	9.1
	$c\parallel$ γ-ray	503	0.47	0.28	4.1
$2a$	$c\perp$ γ-ray	501	0.13	0.34	2.2
	$c\parallel$ γ-ray	494	0.24	0.38	2.1
$2b$	$c\perp$ γ-ray	407	2.28	0.27	3.4
	$c\parallel$ γ-ray	412	0.95[b]	1.03[b]	1.7

[a]Estimated errors in H_{eff}, Δ, and δ (relative to Fe metal) are $\pm$0.0 kOe, $\pm$0.02 mm s^{-1}, and $\pm$0.01 mm s^{-1}, respectively.
[b]Due to the absence of the number 2 and 5 lines, these values are suspect.

rupole interaction in $BaFe_{12}O_{19}$ with that in $SrFe_{12}O_{19}$ and $PbFe_{12}O_{19}$ is problematic, due to the absence of crystal data. However, it is clear that the intrinsic quadrupole splitting for $SrFe_{12}O_{19}$ and $BaFe_{12}O_{19}$ are quite similar, based on the similarity of the apparent values of the polycrystalline samples: 2.27 and 2.30 mm s^{-1} for $SrFe_{12}O_{19}$ and $BaFe_{12}O_{19}$, respectively.[10]

Because the values of the *apparent* quadrupole interaction for the polycrystalline $MFe_{12}O_{19}$ samples are quite close to the *intrinsic* values for the crystals, it is clear that H_{eff} and the electric field gradient are collinear, as expected.

When the c axis is parallel to the γ-ray propagation direction, there are noticeable differences between the spectra of the different hexaferrites (Fig. 3). Although Mössbauer spectra of $MFe_{12}O_{19}$ in this orientation have been

TABLE I. ^{57}Fe hyperfine parameters for single-crystal $PbFe_{12}O_{19}$ at 296 K.

Fe^{3+} site	Crystal alignment	H_{eff}[a] (kOe)	Δ[a] (mm s^{-1})	δ[a] (mm s^{-1})	Relative intensity
$12k$	$c\perp$ γ-ray	412	0.35	0.33	12
	$c\parallel$ γ-ray	414	0.35	0.35	12
$4f_2$	$c\perp$ γ-ray	513	0.29	0.39	4.9
	$c\parallel$ γ-ray	517	0.34	0.39	5.3
$4f_1$	$c\perp$ γ-ray	494	0.11	0.30	4.4
	$c\parallel$ γ-ray	490	0.15	0.26	7.3
$2a$	$c\perp$ γ-ray	486	0.13	0.24	3.8
	$c\parallel$ γ-ray	505	0.06	0.36	3.2
$2b$	$c\perp$ γ-ray	398	2.00	0.30	2.2
	$c\parallel$ γ-ray	415	2.45	0.43	0.9

[a]Estimated errors in H_{eff}, Δ, and δ (relative to Fe metal) are $\pm$1 kOe, $\pm$0.02 mm s^{-1}, and $\pm$0.01 mm s^{-1}, respectively.

TABLE III. ^{57}Fe hyperfine parameters for single-crystal $BaMn_{0.3}Fe_{11.7}O_{19}$ at 296 K.

Fe^{3+} site	Crystal alignment	H_{eff}[a] (kOe)	Δ[a] (mm s^{-1})	δ[a] (mm s^{-1})	Relative intensity
$12k$	$c\perp$ γ-ray	413	0.47	0.38	12
	$c\parallel$ γ-ray	411	0.52	0.36	12
$4f_2$	$c\perp$ γ-ray	508	0.35	0.50	5.5
	$c\parallel$ γ-ray	509	0.48	0.44	5.8
$4f_1$	$c\perp$ γ-ray	482	0.53	0.25	4.7
	$c\parallel$ γ-ray	485	0.45	0.30	7.1
$2a$	$c\perp$ γ-ray	497	0.37	0.31	3.1
	$c\parallel$ γ-ray	503	0.20	0.43	3.6
$2b$	$c\perp$ γ-ray	402	2.29	0.31	2.1
	$c\parallel$ γ-ray	...	...	...	0

[a]Estimated errors in H_{eff}, Δ, and δ (relative to Fe metal) are $\pm$2 kOe, $\pm$0.02 mm s^{-1}, and $\pm$0.01 mm s^{-1}, respectively.

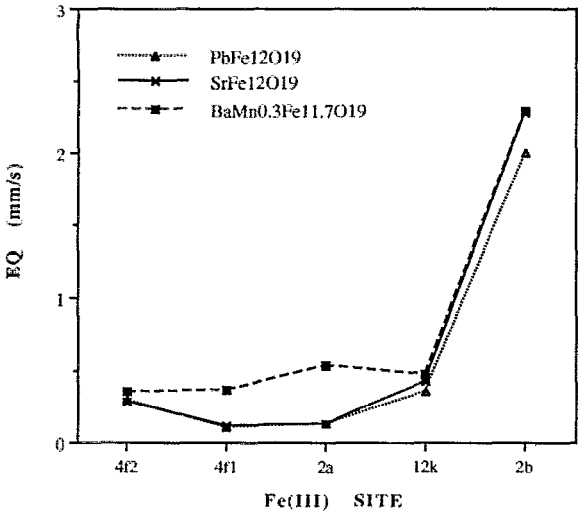

FIG. 2. Plot of Fe^{3+} site vs quadrupole interaction for $MFe_{12}O_{19}$ at 296 K (c axis perpendicular to γ-ray beam).

collected before, only now have quantitative differences been observed between the hexaferrites. It had previously been assumed that the hexaferrites exhibited similar anisotropies.

As is evident in Tables I and II, the relative intensity of the $2b$ subspectrum is clearly greater in $SrFe_{12}O_{19}$ than in $PbFe_{12}O_{19}$. This smaller relative intensity indicates that the $2b$ Fe^{3+} ion exhibits a significantly greater displacement parallel to the c axis in $PbFe_{12}O_{19}$ than in $SrFe_{12}O_{19}$. For the $BaMn_{0.3}Fe_{11.7}O_{19}$ crystal, the low signal-to-noise ratio of the spectrum prevents any conclusions from being drawn about the displacement of the $2b$ Fe^{3+} ion in $BaFe_{12}O_{19}$. But based on the relative intensity of the $2b$ subspectra in the polycrystalline and perpendicularly oriented $MFe_{12}O_{19}$ samples, the $2b$ Fe^{3+} vibrational anisotropy of $BaFe_{12}O_{19}$ is expected to be very similar to that of $SrFe_{12}O_{19}$.

IV. CONCLUSION

Analysis of the ^{57}Fe Mössbauer hyperfine parameters for oriented single crystals have allowed the submicroscopic structure of the M-type hexaferrites to be related to their bulk magnetic properties. Only the $2b$ quadrupole interaction varies significantly between the three hexaferrites, suggesting that the oscillation parallel to the c axis of the $2b$ Fe^{3+} ion is the most important factor in determining the differences in their bulk magnetic behavior.

Based on the relative intensities of the $2b$ subspectra for crystals with the c axis parallel to the γ ray, a tentative ranking of the anisotropy in the displacement of the $2b$ Fe^{3+} ion in the $MFe_{12}O_{19}$ group can be inferred: $PbFe_{12}O_{19} > SrFe_{12}O_{19} \approx BaFe_{12}O_{19}$.

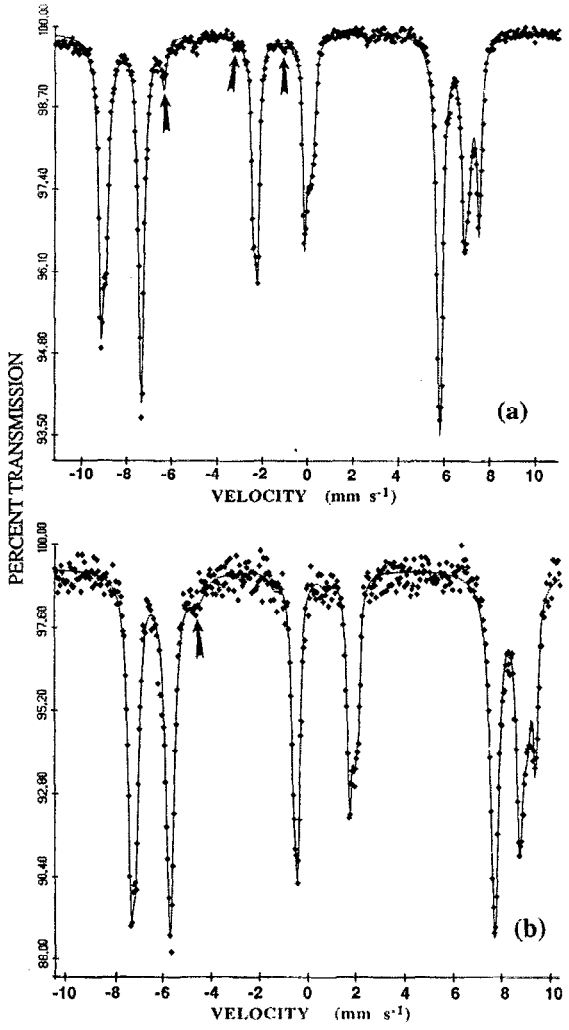

FIG. 3. (a) ^{57}Fe Mössbauer spectrum of single-crystal $SrFe_{12}O_{19}$ (c axis parallel to γ-ray beam) at 296 K. (b) ^{57}Fe Mössbauer spectrum of single-crystal $PbFe_{12}O_{19}$ (c axis parallel to γ-ray beam) at 296 K. Arrows in (a) and (b) indicate the $2b$ subspectrum.

[1] J. G. Rensen and J. S. van Wieringen, Solid State Commun. **7**, 1139 (1969).
[2] E. Kreber, U. Gonser, A. Trautwein, and F. E. Harris, J. Phys. Chem. Solids **36**, 263 (1975).
[3] Y. U. Mamalui, V. P. Romanov, and K. M. Matsievskii, Sov. Phys. Solid State **21**, 117 (1979).
[4] X. Obradors, A. Isalgué, J. Rodríguez, and J. Tejada, Cryst. Lattice Defects Amorph. Mater. **16**, 31 (1987).
[5] J. Fontcuberta, A. Isalgué, and X. Obradors, Z. Phys. B: Condensed Matter **70**, 379 (1988).
[6] J. Fontcuberta and X. Obradors, J. Phys. C: **21**, 2335 (1988).
[7] K. Kimura, M. Ohgaki, K. Tanaka, H. Morikawa, and F. Marumo, J. Solid State Chem. **87**, 186 (1990).
[8] J. Muller and A. Collomb, J. Magn. Magn. Mater. **103**, 194 (1992).
[9] L. Jizhe, Z. Yuchang, J. Hongzhen, and Z. Hongru, Kexue Tongbao **25**, 388 (1980).
[10] G. Thompson and B. Evans, J. Magn. Magn. Mater. **95**, L142 (1991).
[11] B. J. Evans, F. Grandjean, A. P. Lilot, R. H. Vogel, and A. Gérard, J. Magn. Magn. Mater. **67**, 123 (1987).
[12] X. Obradors, A. Collomb, M. Pernet, and J. C. Joubert, J. Magn. Magn. Mater. **44**, 118 (1984).